Interactions of Tides and Mesoscales in a High-Resolution Numerical Ocean Model

Edward D. Zaron, Portland State University, Portland, OR USA

Introduction

MOTIVATION

Do interactions between internal tides (long-wavelength internal gravity waves) and mesoscales (slow balanced motions) play a significant role in either tidal or mesoscale energetics?

ABSTRACT

Output from a high-resolution operational ocean model, AMSEAS, is analyzed to identify interactions between internal tides, which are high-frequency internal gravity waves, and mesoscales, the low-frequency balanced motion, in the Caribbean Sea. Tides are discernable in the SSH at scales smaller than 150km, with contributions from both the stationary (coherent, phase-locked) and non-stationary (incoherent) internal tides. Dynamical interactions are analyzed by decomposing the velocity field into three components: a low-frequency mesoscale, coherent tides, and a high-frequency residual, and evaluating the Reynolds stresses from the residual. An initial analysis at a number of sites finds that the lateral Reynolds stress in the tidal band are not related to the mesoscale rate of strain. However, a correlation between the mesoscale strain rate and the amplitude of the non-stationary tide is found, which provides indirect evidence for tide–mesoscale interactions.

The AMSEAS Model

- 3km-resolution implementation of the Navy Coastal Ocean Model (NCOM), covering the Gulf of Mexico, Caribbean Sea, and Western Atlantic.
- 55 vertical layers – sigma levels down to 550m and z-levels below that to 5000m.
- The one-year period, June 2010 through June 2011, used here.
- Air-sea fluxes (COAMPS), barotropic tides (OTIS), and baroclinic open-boundary conditions (Global NCOM) are used to force the model.
- 96-hour forecasts produced daily with output archived at 3-hour intervals.

Analysis Methods

- **Stationary Tides** are computed via harmonic analysis of 1 year of model outputs at 8 dominant tidal frequencies.
- **Non-Stationary Tides** are computing by subtracting stationary tides and performing harmonic analysis of diurnal and semidiurnal bands within 96-hour windows.
- **Causes of Non-Stationary Tides** are inferred from

$$\frac{1}{2}\frac{\delta c_0^2}{c_0^2} + Fr + \frac{1}{2}\frac{f^2}{\omega^2}Ro,$$

refraction by time-varable stratification (δc_0), Doppler shifting (Froude number, Fr), and refraction by relative vorticity (Ro).
- **Potential for Tide-Mesoscale Interactions** is measured by

$$I = \frac{S_0}{2}(\omega^2 - f_e^2)\cos 2(\phi - \theta)$$

where $S_0^2 = a^2 + b^2$ is the squared rate of strain, defined in terms of $a = \overline{u}_x - \overline{v}_y$ and $b = \overline{v}_x + \overline{u}_y$; ω is the tidal frquency; $f_e = f(1 + Ro/2)$ is the effective Coriolis frequency; and $\phi - \theta$ is the angular difference between the principal axis of the rate-of-strain matrix ($\phi = \tan^{-1}(b/a)$) and the direction of propagation of the tide.
- **Reynolds Stresses**, $\tau_{ij} = -\langle u_i u_j \rangle$, are computed by decomposing the flow into 96-hour average ($\overline{u}, \overline{v}$), stationary tides ($\hat{u}, \hat{v}$), non-staionary tides ($u^t, v^t$), and a residual ($u', v'$).

Observed and Modeled SSH and Tides

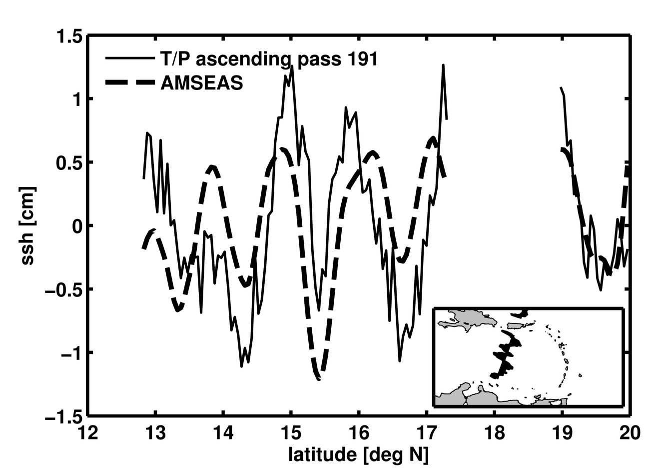

Figure 1: Surface expression of M_2 internal tide along TOPEX pass 191.

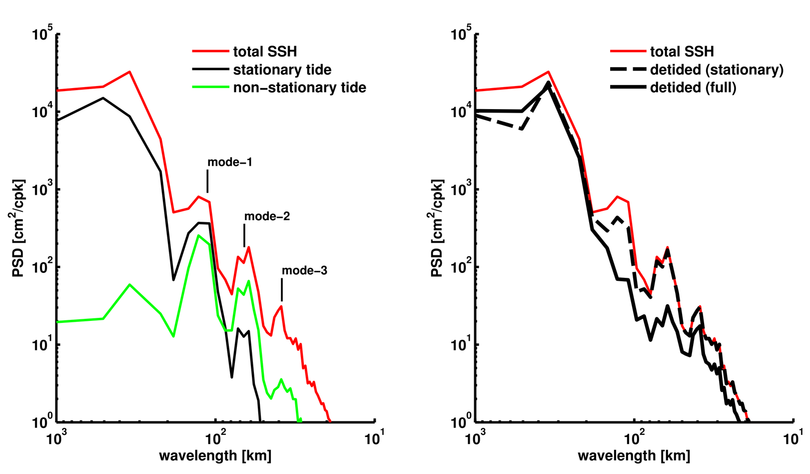

Figure 2: Radial wavenumber spectrum, AMSEAS.

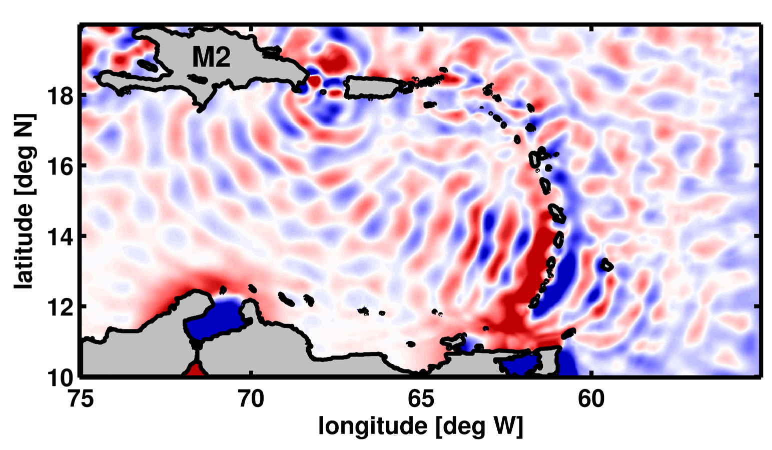

Figure 3: AMSEAS stationary M_2 internal tide (quadrature component). Color scale from -3cm (blue) to $+3$cm (red).

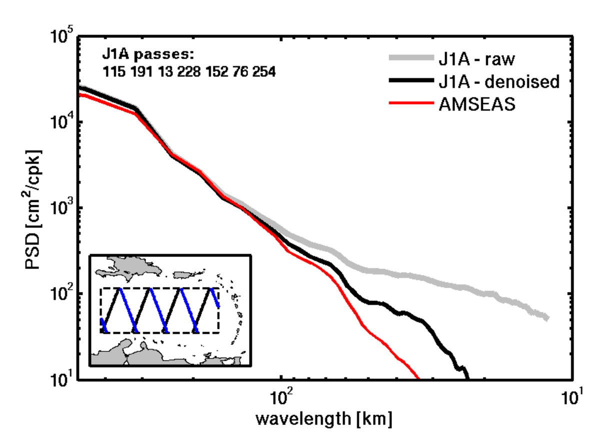

Figure 4: AMSEAS vs. JASON-1 altimeter wavenumber spectra, based on data from 2002–2009.

Non-Stationary Tides

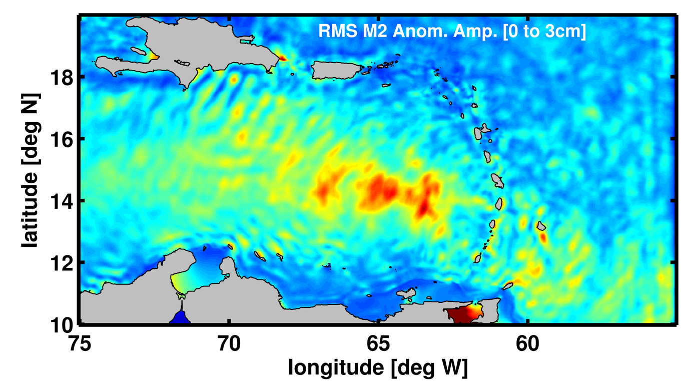

Figure 5: Non-stationary M_2 amplitude

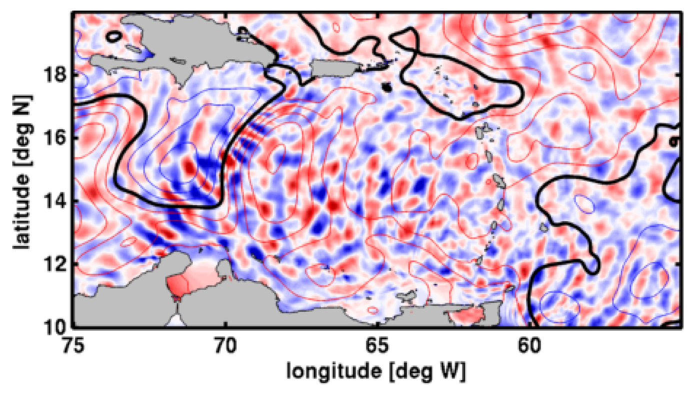

Figure 6: Possible interaction of internal tide and mesoscale, near 70° W. Non-stationary M_2 SSH is shown with contours of mesoscale SSH overlaid.

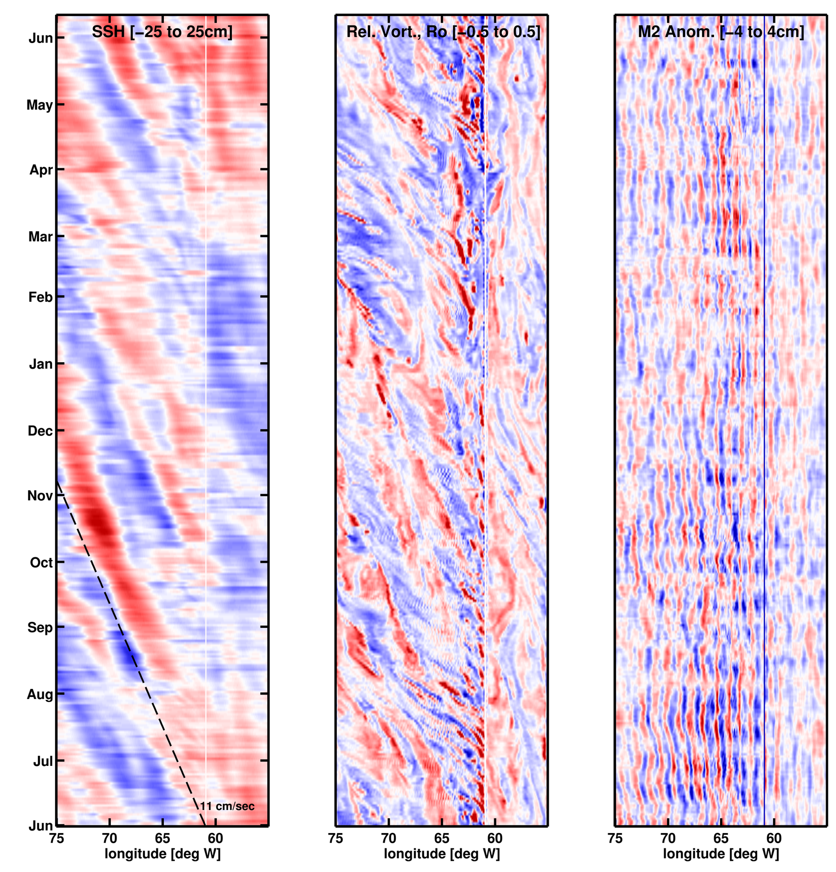

Figure 7: Hovmöller diagram for 2010–2011 across 14°N: subtidal SSH (left), geostrophic relative vorticity (center), quadrature component of non-stationary tide (right).

Tide-Mesoscale Interactions Diagnosed from the Rate-of-Strain Tensor

Stability analysis of a plane wave propagating through a non-divergent flow field indicates a growth rate proportional to the rate of strain, S_0. Is there a correlation between S_0 and the non-stationary internal tide?

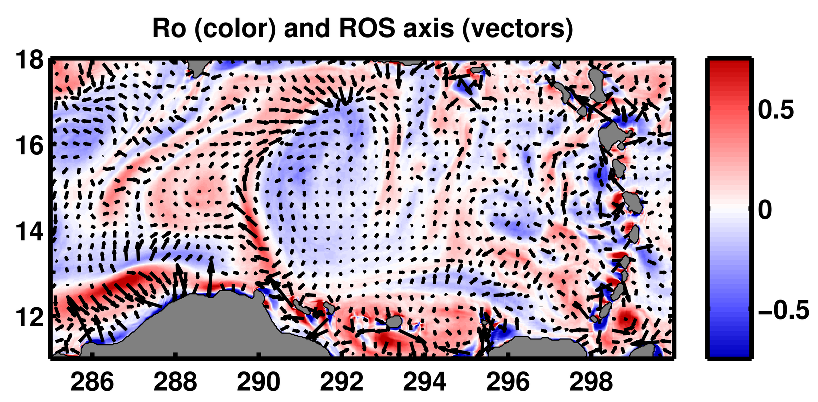

Figure 8: Rossby number and principal axis of rate-of-strain tensor.

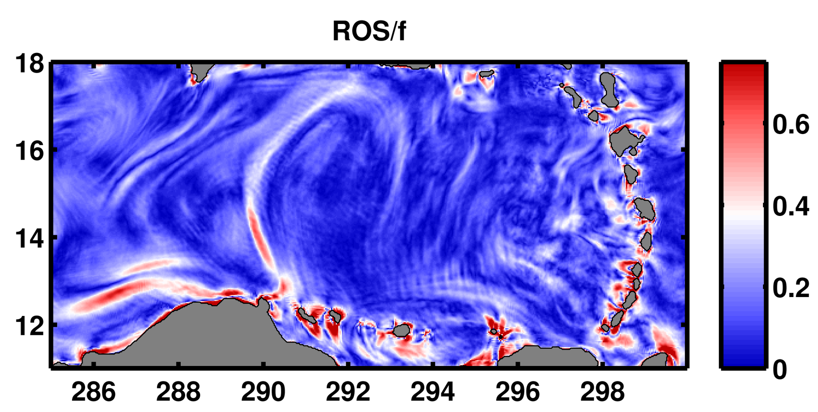

Figure 9: Snapshot of S_0/f, the rate of strain normalized by the Coriolis parameter.

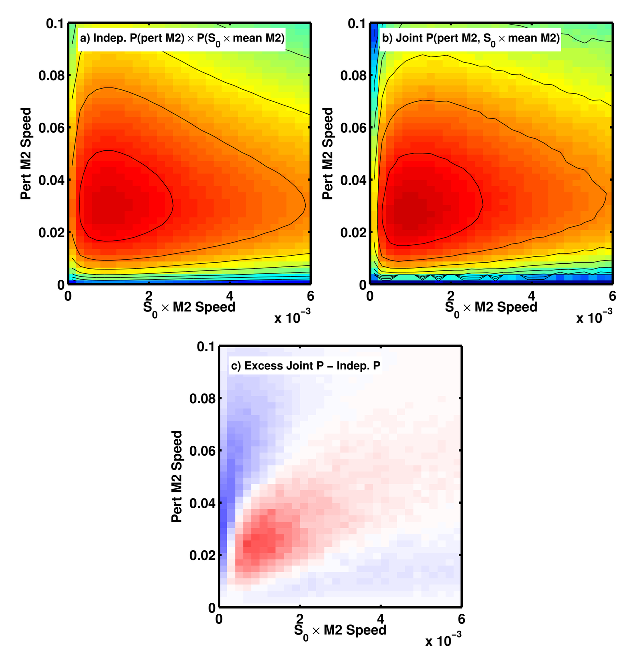

Figure 10: Two-dimensional probability density functions (pdfs), A^t_{M2} versus $S_0\hat{A}_{M2}$. a) The product of the univariate pdfs illustrates the null-hypothesis. b) The sample pdf. c) Difference between (b) and (a) indicates correlation between A^t_{M2} and $S_0\hat{A}_{M2}$.

Reynolds Stresses

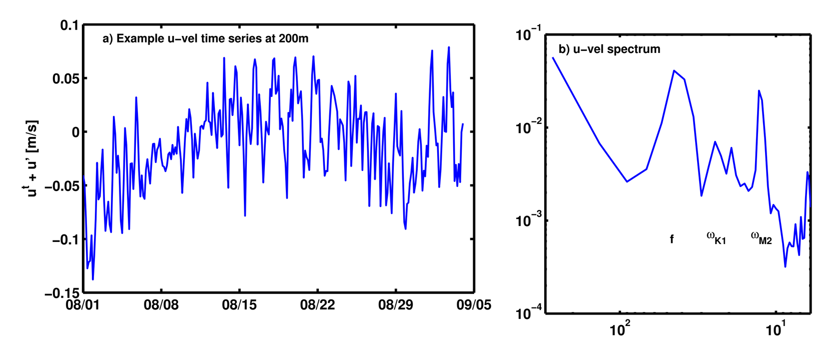

Figure 11: Representative de-tided u-velocity (a) time series and (b) power spectrum shows intermittency of currents and prominence of near-inertial variability.

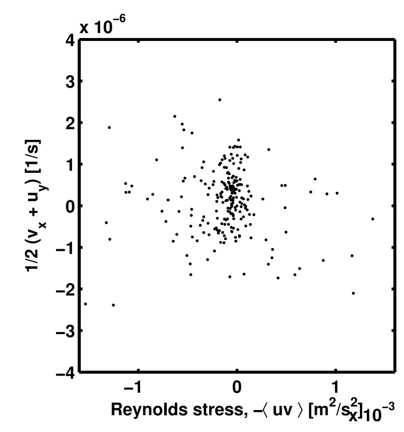

Figure 12: No statistically significant relation between Reynolds stress and the rate of strain has been found.

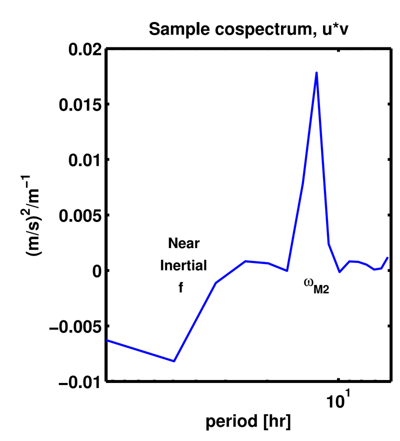

Figure 13: Both near-inertial motion and non-stationary tides contribute significantly to the Reynolds stress.

Conclusions

- Stationary and non-stationary tides have been examined in the AMSEAS model.
- A correlation between the mesoscale rate-of-strain and non-stationary tidal currents has been found.
- Direct evidence of nonlinear interactions diagnosed from Reynolds stresses has not been found.
- It is hypothesized that the passively-refracted internal tide signal contaminates the Reynolds stress estimates in the semi-diurnal band.

Acknowledgements

Thanks to the Naval Oceanographic Office and the Northern Gulf Institute for archiving and publishing the AMSEAS model outputs. Satellite altimeter data used here were extracted from the Radar Altimeter Database System (RADS).